*American Mineralogist, Volume 101, pages 2544–2553, 2016*

# Ideal wollastonite and the structural relationship between the pyroxenoids and pyroxenes

**Richard M. Thompson[1,*], Hexiong Yang[2], and Robert T. Downs[2]**

[1]School of Information, University of Arizona, 1103 East 2nd Street, Tucson, Arizona 85721, U.S.A.
[2]Department of Geosciences, University of Arizona, 1040 East 4th Street, Tucson, Arizona 85721, U.S.A.

## Abstract

A hypothetical ideal wollastonite with regular octahedra and T3 tetrahedron is presented and used to compare and contrast the pyroxenes and pyroxenoids. While clinopyroxenes have close-packed arrangements of oxygen anions, several lines of evidence demonstrate that pyroxenoids do not. One such line is the number of tetrahedra in a single tetrahedral chain per octahedra in a single associated octahedral chain (interior to the octahedral band), referred to as the "single-chain T:O ratio," which is 1:1 in pyroxenes but 3:2 in wollastonite and always greater than 1:1 in other $MSiO_3$ pyroxenoids. Because the Si-tetrahedron is extremely resistant to distortion, this forces marked distortion in at least one pyroxenoid octahedral site.

The octahedral layers in pyroxenes and pyroxenoids are compared by placing them in the context of a fully occupied, closest-packed sheet of idealized octahedra, and it is shown that they are fundamentally different.

The new mineral yangite is analyzed from the perspective developed in this study. It is structurally similar to the pyroxenoids, but the structure is a new type because it contains double tetrahedral chains and mixed polyhedral layers containing double chains of tetrahedra and bands of octahedra of width two. The tetrahedral chains are wollastonite-type chains and the wollastonite-type double chain is shown to have important differences from the amphibole double chain. A possible explanation for the existence of this crystal structure based on a hydrogen bond between Pb and O is presented.

**Keywords:** Clinopyroxene, pyroxenoid, chain silicate, yangite, wollastonite, diopside, close-packing

## Introduction

The new mineral yangite, a new type of chain silicate with double tetrahedral chains and ideal formula $PbMnSi_3O_8 \cdot H_2O$, is described elsewhere in this issue (Downs et al. 2016). This companion paper compares and contrasts the pyroxenoids and pyroxenes to develop some new approaches to characterizing and understanding members of the pyroxenoid group. To do so, this study compares hypothetical ideal pyroxenoids and pyroxenes—specifically the relationships between their tetrahedral and octahedral structural subunits, their anion packing arrangements, their octahedral arrangements, and the compositions of their "polyhedral layers," as defined below. The octahedral arrangement of a hypothetical pyroxenoid with T-chain repeat unit length of 11 is predicted. Finally, the new approaches are applied to see how yangite compares with the pyroxenoids and provide an understanding of why its structure is adopted.

Numerous papers have discussed the structural relationship between the pyroxenes and pyroxenoids, with a particular emphasis on the description of pyroxenoids as polysomes built from pyroxene and "wollastonite-like" (Angel and Burnham 1991) modules. By the 1980s, it was known that clinopyroxene (Cpx) and pyroxenoid (Pxd) intergrowths take place along face poles $(1\bar{1}\bar{1})$ and (001) in Cpx and Pxd, respectively (cf. Ried 1984). During that decade, the existence of isostructural portions of the two structures that would allow seamless intergrowth was debated. By the early 1990s, it was determined that such portions did exist (cf. Veblen 1991; Angel and Burnham 1991). Figures 1a and 1b illustrate isostructural planar portions of diopside (Thompson and Downs 2008) and rhodonite (Peacor et al. 1978), looking down face poles $(1\bar{1}\bar{1})$ and (001), respectively.

Many other discussions of the relationship between the pyroxenes and pyroxenoids focus on tetrahedral chain (T-chain) geometry and repeat length because T-chain repeat length in described pyroxenoids is variously 3, 5, 7, or 9 (cf. Klein and Dutrow 2008). Prewitt and Peacor (1964) and Liebau (1956) noted that octahedral cation size determines T-chain type, with decreasing cation size corresponding to increasing T-chain repeat unit length. These topics will be addressed in detail later in the paper. Ohashi and Finger (1978) concluded that the distribution of octahedral cations between the different sites within the octahedral layers determine both structure type and the range of solid solutions. Both Prewitt and Peacor (1964) and Ohashi and Finger (1978) described pyroxenoids as having distorted closest-packed arrangements of oxygen anions.

This report analyzes pyroxenoids and pyroxenes in terms of several different structural subunits, defined here. For the purposes of this paper, a polyhedral layer is a unit that is one polyhedron thick in one direction, called the "stacking vector," and infinite in dimension in all directions perpendicular to the stacking vector. Layered structures, such as the pyroxenoids and pyroxenes, can be described as composed of one or more types

* E-mail: rmthomps@email.arizona.edu

0003-004X/16/0011–2544$05.00/DOI: http://dx.doi.org/10.2138/am-2016-5683

of polyhedral layer stacked along the stacking vector in a finite sequence that repeats infinitely. Polyhedral layers can be used to orient related structures for comparison.

This approach is a natural extension of the concept that some crystal structures are based on close-packing of oxygen atoms. The polyhedral layers described below for diopside (and all clinopyroxenes) each consist of cations sandwiched between two adjacent close-packed oxygen monolayers (Thompson and Downs 2003). Similarly, the pyroxenoid polyhedral layers analyzed in this paper consist of cations between two adjacent oxygen monolayers, although we will present evidence that these monolayers should not be considered close-packed. Selecting polyhedral layers that are bounded by oxygen monolayers (close-packed or not) constrains them to be one polyhedron in thickness and to consist of polyhedra that each have at least one "basal face," a face approximately parallel to the polyhedral plane (perpendicular to the stacking vector).

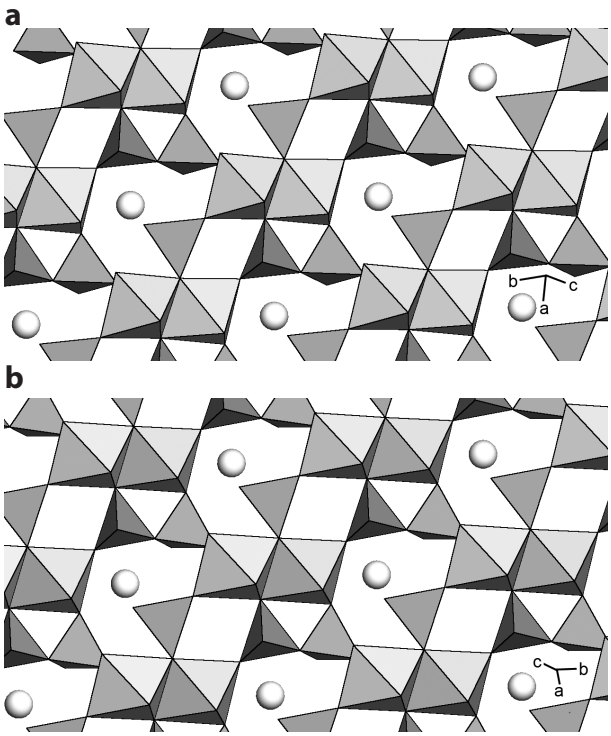


**FIGURE 1.** (**a**) Diopside (Thompson and Downs 2008) viewed down face pole ($1\bar{1}\bar{1}$). (**b**) Rhodonite (Peacor et al. 1978) viewed down face pole (001).

Figure 2 is a cartoon of diopside (Thompson and Downs 2008), wollastonite-1*A* (Ohashi and Finger 1978), and yangite (Downs et al. 2016) viewed perpendicular to their stacking vectors (looking at the polyhedral layers edge on) to illustrate the best alignment of the structures for comparison. This view is chosen so that the "tilt" of the octahedra (cf. Thompson 1970; Papike et al. 1973; Thompson and Downs 2003) in each of the structures is evident and in alignment.

From this perspective, the layered nature of the structures is obvious, with five polyhedral layers visible in each representation. Each polyhedral layer in diopside, wollastonite, and the other well-known pyroxenoids analyzed in this paper contains either octahedra or tetrahedra, but not both. Such layers are hereafter referred to as "isopolyhedral layers." Layers such as those in yangite that contain more than type of polyhedron will be referred to as "mixed polyhedral layers."

Figure 3 is a cartoon of yangite viewed down **b**. From this angle, the structure could be considered to be constructed from alternating layers of tetrahedra and octahedra. However, these layers do not fit our definition of polyhedral layer because they are undulating and therefore more than one polyhedron thick, are not bounded by oxygen monolayers, contain polyhedra without basal faces, and do not provide a natural basis for comparison with pyroxenes and previously described pyroxenoids.

This study also uses idealized models of the octahedral layers of pyroxenes and pyroxenoids to highlight similarities and differences instead of polysomatic construction or T-chain geometry. Octahedral layers in pyroxenoids are composed of linear structural subunits that are several octahedra wide and infinitely long. Prior authors (cf. Weber 1983) have referred to these edge-sharing arrangements as "bands," and this paper continues that practice.

Additionally, we will specifically focus on a single edge-sharing octahedral chain (referred to hereafter as the "O-chain") interior to the octahedral band in each of $Ca_{0.96}Mn_{0.04}SiO_3$ wollastonite-1*A* (Ohashi and Finger 1978), $Mn_{0.71}Mg_{0.17}Ca_{0.12}SiO_3$

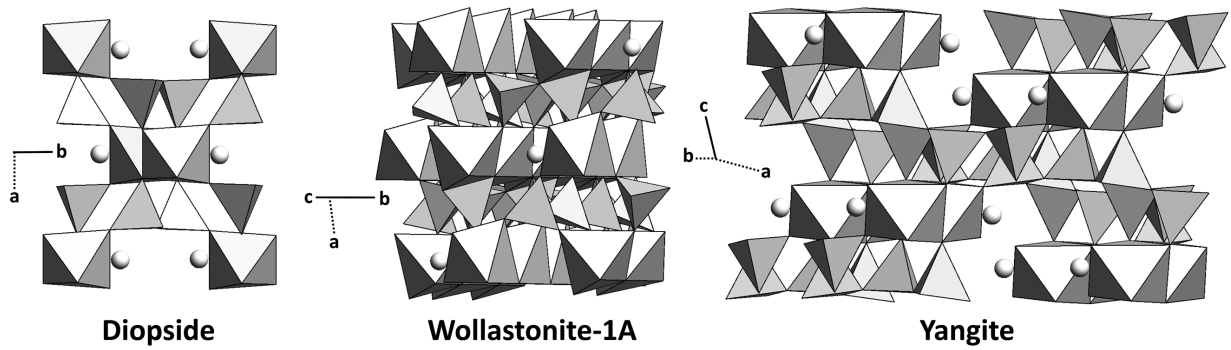


**FIGURE 2.** The structures of diopside (Thompson and Downs 2008), wollastonite-1*A* (Ohashi and Finger 1978), and yangite (Downs et al. 2016) viewed so that "tilt" of the octahedra (cf. Thompson 1970; Papike et al. 1973; Thompson and Downs 2003) in each of the structures is evident and in alignment.

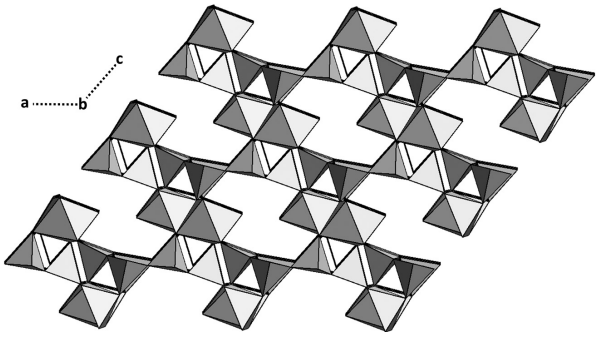


**FIGURE 3.** Yangite viewed down **b**.

rhodonite (Peacor et al. 1978), $Mn_{0.92}Mg_{0.08}SiO_3$ pyroxmangite (Zanazzi et al. 2008), and $FeSiO_3$ ferrosilite III (Weber 1983). Figures 4a–4d illustrate the O-chains within the band of octahedra in each of these minerals. Figure 5 isolates and idealizes the chains, placing them adjacent to each other to highlight the stepwise progression from wollastonite through the other pyroxenoids toward the pyroxene configuration.

Analyzing the O-chain instead of the entire octahedral band makes it easier to focus on the key patterns and differences among these pyroxenoids. It also allows direct comparison between each of the pyroxenoids and the pyroxene O-chain by placing them in the context of a fully occupied, closest-packed sheet of idealized octahedra, hereafter referred to as a "brucite-type layer," following common practice. Finally, it allows us to define the "single-chain T:O ratio" as the ratio of the length of the T-chain repeat length to the O-chain repeat length, a useful parameter.

This study begins with a focus on wollastonite-1*A* (Ohashi and Finger 1978), for which we present a complete idealized hypothetical crystal structure data set, because of its relative simplicity in the sense that it contains only isopolyhedral layers, because its octahedral band geometry is comparatively straightforward as detailed below, and because its T-chain repeat length is the pyroxenoid minimum of three. It is also an end-member composition in the chemical continuum of crystals with general formula $MXO_3$, where the M-site(s) are occupied by one or more of several different metallic elements and X-site elements can be C, Si, Ge, B, or Al in either tetrahedral or trigonal coordination. End-member compositions are particularly useful because they help elucidate the role of cation size in determining structure.

## DISCUSSION

Pyroxenoids are often described as similar to the pyroxene group because both groups contain chains of corner-sharing $SiO_4$ tetrahedra connected to chains of octahedrally coordinated cations, but distinguished by their T-chain geometry (cf. Klein and Dutrow 2008). Specifically, pyroxenoid T-chains have a repeat unit that is three or more tetrahedra long, as opposed to the two-tetrahedra periodicity in pyroxenes (cf. Merlino and Bonaccorsi 2008).

However, the pyroxene and pyroxenoid structures are fundamentally different in several other respects, including O-chain geometry, anion packing, and the relationship between their T- and O-chains. Tables 1 and 2 contain cell and positional parameters for a hypothetical ideal wollastonite-1*A* with the $C\bar{1}$ structure of Ohashi and Finger (1978), but constrained to have regular octahedra and T3 tetrahedron (the ideal T-site cation corresponding to the observed Si3 atom; Fig. 6). These requirements fix the positions of all oxygen atoms except Oc1 [see Fig. 6; oxygen atom names follow Ohashi and Finger (1978), which will be the reference for observed wollastonite hereafter].

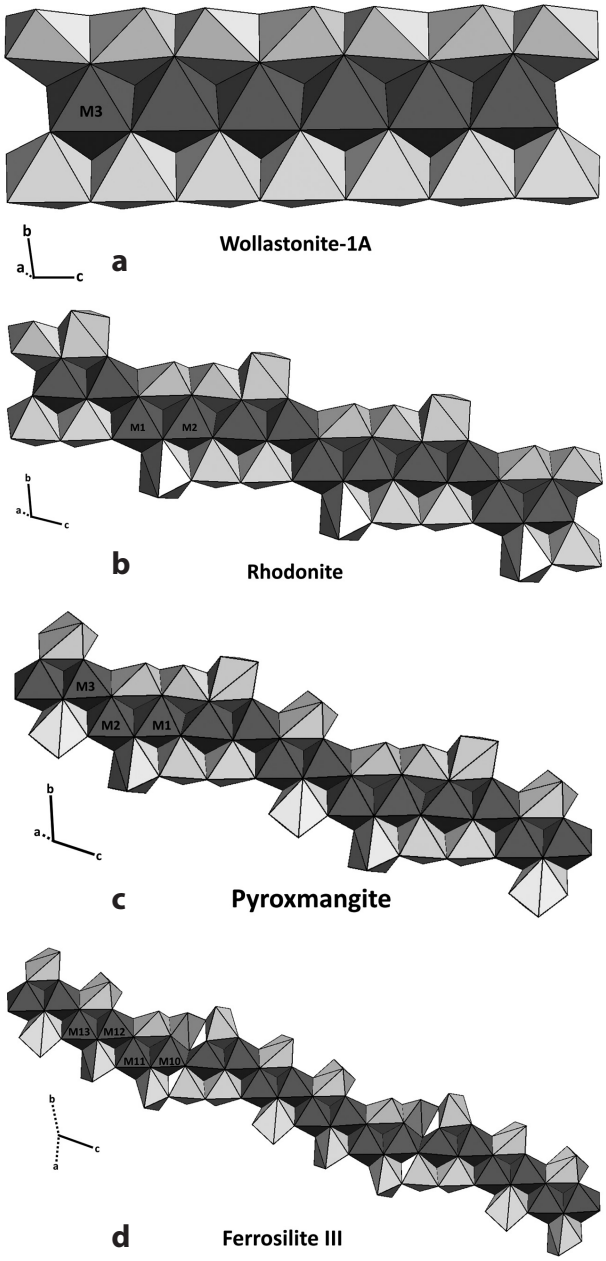


**FIGURE 4.** The edge-sharing "O-chain" in four pyroxenoids, each of which has different T-chain repeat length. The O-chain is interior to the octahedral band and is highlighted in Figures 2a–2d as darker octahedra. (**a**) Wollastonite-1*A* (Ohashi and Finger 1978), (**b**) rhodonite (Peacor et al. 1978), (**c**) pyroxmangite (Zanazzi et al. 2008), and (**d**) ferrosilite III (Weber 1983) have T-chain repeat lengths of 3, 5, 7, and 9, respectively.

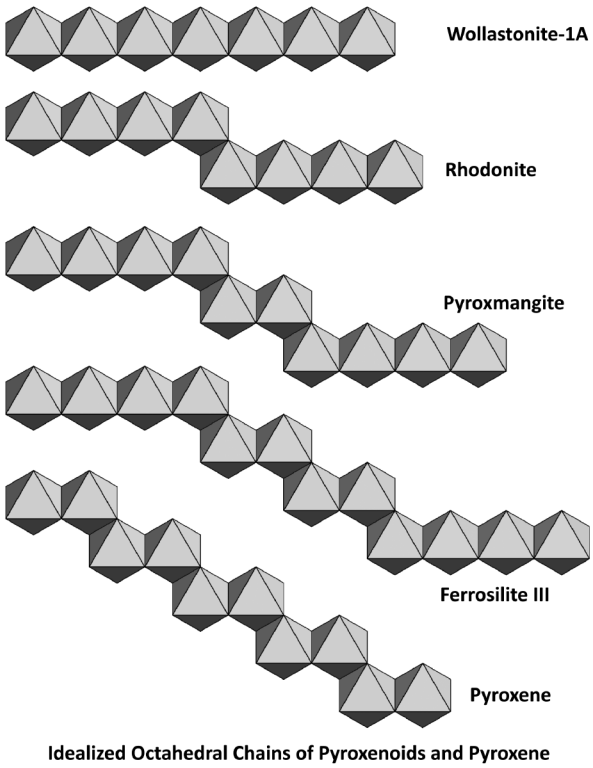


**FIGURE 5.** Idealized versions with regular octahedra of the O-chains in wollastonite-1*A* (Ohashi and Finger 1978), rhodonite (Peacor et al. 1978), pyroxmangite (Zanazzi et al. 2008), ferrosilite III (Weber 1983), and pyroxene (Thompson and Downs 2003).

**TABLE 1.** Cell parameters for a hypothetical ideal wollastonite with regular octahedra and the corresponding observed structure (Ohashi and Finger 1978)

| | Ideal wollastonite | $r$ = 1.58982 Å | Ohashi and Finger (1978) |
|---|---|---|---|
| $a$ (Å) | $2\sqrt{11}r$ | 10.546 | 10.104(1) |
| $b$ (Å) | $\frac{2}{3}\sqrt{129}r$ | 12.038 | 11.054(1) |
| $c$ (Å) | $4r$ | 6.359 | 7.305(1) |
| α (°) | $\cos^{-1}[-3/(2\sqrt{129})]$ | 97.59 | 99.53(1) |
| β (°) | $\cos^{-1}[-4/(8\sqrt{11})]$ | 98.67 | 100.56(1) |
| γ (°) | $\cos^{-1}(4/\sqrt{1419})$ | 83.90 | 83.44(1) |
| $V$ (Å$^3$) | $416\sqrt{2}r^3/3$ | 788.0 | 788.0(1) |

*Notes:* Ideal parameters are given exactly and as a decimal approximation. Exact parameters are expressed in terms of $r$, where $r$ = one-half the octahedral edge length. Space group is $C\bar{1}$.

**TABLE 2.** Positional parameters for ideal and observed wollastonite

| | Ideal | Ideal | O&F |
|---|---|---|---|
| M1 | 0 | 0 | 0.0212 |
| | 19/26 | 0.7308 | 0.7800 |
| | 3/52 | 0.0577 | 0.0772 |
| M2 | 0 | 0 | 0.0180 |
| | 19/26 | 0.7308 | 0.7803 |
| | 29/52 | 0.5577 | 0.5712 |
| M3 | 0 | 0 | 0.0137 |
| | 1/2 | 0.5 | 0.4889 |
| | 1/4 | 0.25 | 0.2504 |
| T1 | 3/16 | 0.1875 | 0.2265 |
| | 197/208 | 0.9471 | 0.9585 |
| | 173/208 | 0.8317 | 0.8876 |
| T2 | 3/16 | 0.1875 | 0.2266 |
| | 197/208 | 0.9471 | 0.9576 |
| | 101/208 | 0.4856 | 0.4540 |
| T3 | 3/16 | 0.1875 | 0.2260 |
| | 37/208 | 0.1779 | 0.1711 |
| | 45/208 | 0.2163 | 0.2237 |
| Oa1 | 1/8 | 0.125 | 0.1164 |
| | 59/104 | 0.5673 | 0.5786 |
| | 5/104 | 0.0481 | 0.0381 |
| Oa2 | 1/8 | 0.125 | 0.1168 |
| | 59/104 | 0.5673 | 0.5807 |
| | 57/104 | 0.5481 | 0.5612 |
| Oa3 | 1/8 | 0.125 | 0.1149 |
| | 35/104 | 0.3365 | 0.3142 |
| | 77/104 | 0.7404 | 0.7305 |
| Ob1 | 1/8 | 0.125 | 0.1248 |
| | 83/104 | 0.7981 | 0.8577 |
| | 89/104 | 0.8558 | 0.8750 |
| Ob2 | 1/8 | 0.125 | 0.1239 |
| | 83/104 | 0.7981 | 0.8567 |
| | 37/104 | 0.3558 | 0.3657 |
| Ob3 | 1/8 | 0.125 | 0.1147 |
| | 35/104 | 0.3365 | 0.2874 |
| | 25/104 | 0.2404 | 0.2271 |
| Oc1 | 1/8 | 0.125 | 0.2201 |
| | 99/104 | 0.9519 | 0.9955 |
| | 67/104 | 0.6442 | 0.6780 |
| Oc2 | 1/8 | 0.125 | 0.1811 |
| | 11/104 | 0.1058 | 0.0887 |
| | 45/104 | 0.4327 | 0.3703 |
| Oc3 | 1/8 | 0.125 | 0.1823 |
| | 11/104 | 0.1058 | 0.0912 |
| | 97/104 | 0.9327 | 0.0119 |

*Note:* Ohashi and Finger (1978) did not report errors with their positions.

Oc1 is placed so all oxygen atoms form coplanar layers stacked perpendicular to **a***, and T1 and T2 have identical geometries. While this choice is arbitrary, there is no placement of Oc1 that would result in a complete structure with all regular polyhedra, as would be the case if the anion skeleton of wollastonite were a distorted close-packed arrangement. This hypothetical idealized wollastonite will be used for comparison with observed wollastonite and ideal and observed diopside (Thompson and Downs 2008), arbitrarily chosen as a representative pyroxene.

Figure 6 is a cartoon of the relationship between the wollastonite-1*A* T- and O-chains, which are composed of a single type of octahedron (M3), illustrated for observed and ideal wollastonite viewed down **a*** and for the most analogous portion of a hypothetical closest-packed crystal. It is evident that there is no closest-packed model that directly corresponds with the wollastonite structure. Closest-packing creates characteristic arrangements of tetrahedral and octahedral interstitial sites. If the cation coordination polyhedra in a mineral cannot be mapped to corresponding sites in a closest-packed arrangement with an identical bonding topology, the mineral should not be considered as having a close-packed arrangement of anions.

By inspection of Figure 6, the single-chain T:O ratio is three tetrahedra in the T-chain for every two O-chain octahedra, but in a close-packed mineral (like pyroxene; Thompson 1970; Thompson and Downs 2003) this ratio is 1:1. This creates an unusual geometry for T1 and T2 in the ideal wollastonite. T3 shares edges with M1 and M2 octahedra, and constraining the octahedra to be regular constrains T3 geometry to also be regular. Therefore, the mismatch in the single-chain T:O ratio relative to closest-packing (which allows all polyhedra to be regular) must be accommodated by T1 and T2 in the hypothetical structure, and they deviate markedly from regular.

In reality, Si tetrahedra are extremely resistant to distortion and in observed wollastonite the octahedral sites Ca1 and Ca2 are

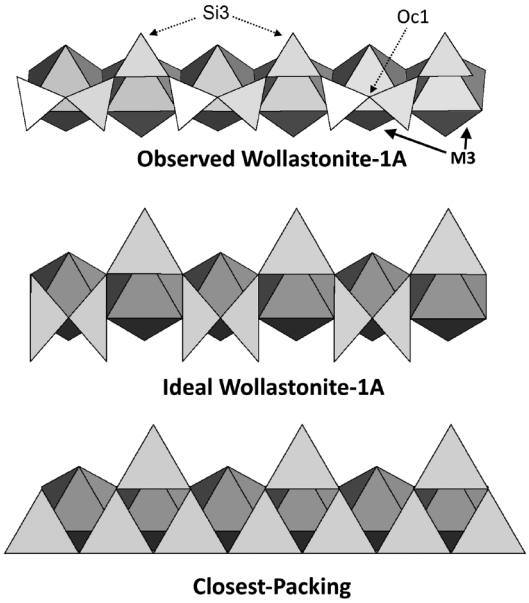


**FIGURE 6.** The relationship between the T- and O-chains in observed and ideal wollastonite-1*A*, viewed down **a***, and the most analogous portion of a hypothetical closest-packed crystal. There are three tetrahedra for every two octahedra with which the tetrahedra share apical corners, greater than the closest-packed ratio of 1:1 and a demonstration that wollastonite is not a close-packed mineral. Observed wollastonite is from Ohashi and Finger (1978).

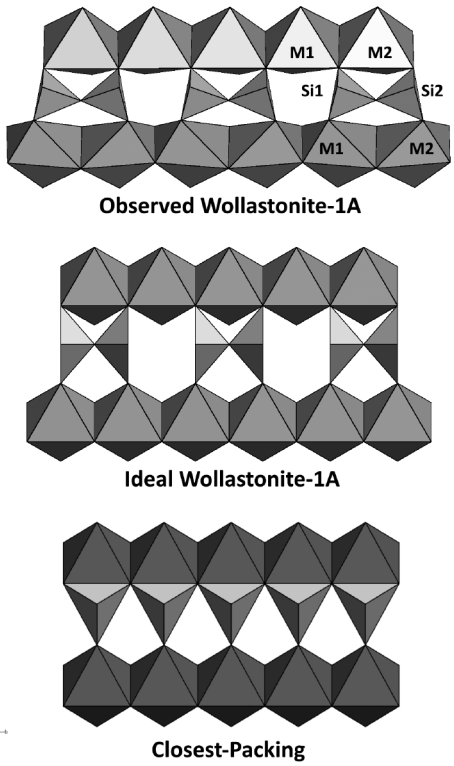


**FIGURE 7.** A comparison of T1 and T2 bridging the O-chains in observed (Ohashi and Finger 1978) and ideal wollastonite-1*A*, viewed down **a***, and the most analogous portion of a hypothetical closest-packed crystal. Si-tetrahedra are extremely resistant to distortion, and the octahedra in observed wollastonite distort to allow the tetrahedra to become more regular.

quite distorted allowing T-sites Si1 and Si2 to be nearly regular. Si3 is the most distorted tetrahedron, but is still more regular than M3 and much less distorted than M1 and M2.

Figure 7 shows a view down **a*** of the bridging tetrahedra in observed and ideal wollastonite along with the O-chains that they connect. It also illustrates a portion of a hypothetical closest-packed crystal with occupancies chosen to provide the nearest possible correspondence to the wollastonite diagrams. Si3 bridges Si1 and Si2 (Fig. 6) but is not shown so that the octahedra are fully visible. Taking into account the missing $Si_3$, there are three tetrahedra in the T-chain for every two octahedra in the adjacent octahedral chains, one more than is possible in a closest-packed arrangement.

It is evident that the octahedra are distorted to accommodate the extra T site. The two pictured O-chains are composed of alternating M1 and M2 sites. Table 3 contains polyhedral angle variance values for the polyhedra in observed wollastonite, a traditional measure of polyhedral distortion (Robinson et al. 1971) such that a regular polyhedron has a value of zero and larger values indicate greater distortion. Table 3 shows that Ca1 and Ca2 are much more distorted than Si1 and Si2, accommodating the high T:O ratio.

Additionally, Figure 7 again demonstrates that there is no closest-packed model that directly corresponds with the wollastonite structure.

While any idealized pyroxenoid O-chain taken in isolation can be placed into a brucite-type layer (see below), two or more idealized octahedral bands cannot without altering their relative positions. Figure 8 is a cartoon of a portion of an ideal wollastonite octahedral layer viewed down **a***. The darker octahedra are M3 and the dotted arrows indicate a minimum translation the lower octahedral band would have to undergo relative to the upper octahedral band to be closest-packed.

**TABLE 3.** Polyhedral angle variance (Robinson et al. 1971) values for Ca1, Ca2, T1, and T1 in observed wollastonite (Ohashi and Finger 1978)

| Site | Ca | Si |
|---|---|---|
| 1 | 176.8 | 26.2 |
| 2 | 177.1 | 22.1 |
| 3 | 95.7 | 60.0 |

*Notes:* A value of zero indicates a regular polyhedron, higher values indicate increasing distortion. The O-sites are much more distorted than the T-sites.

We now compare and contrast the pyroxenoid and pyroxene O-chains by placing them in the context of a closest-packed brucite-type octahedral layer.

Figure 6 included the M3 O-chain in observed and ideal wollastonite; Figure 9a illustrates the M1 O-chain in observed and ideal diopside, looking down **a*** with the O-chains running parallel to **c**. Figure 9b illustrates the relationship between the wollastonite and pyroxene O-chains by placing them in the context of a brucite-type layer. There are three ways to orient a pyroxene O-chain in a brucite-type layer relative to a wollastonite O-chain: two with pyroxene **c** axis at 30° to the wollastonite **c** axis and one with the axes perpendicular. Figure 9b shows one

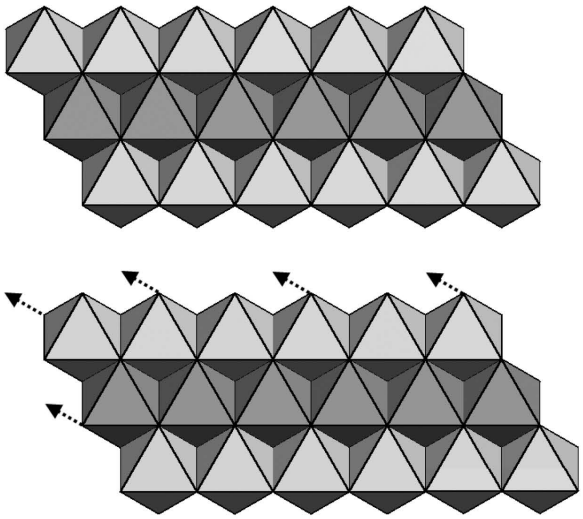

**FIGURE 8.** A portion of the ideal wollastonite-1*A* octahedral layer, viewed down **a***. M3 octahedra are darker. The arrows indicate a minimum translation necessary to make the layer closest-packed, again demonstrating that wollastonite is not a close-packed mineral.

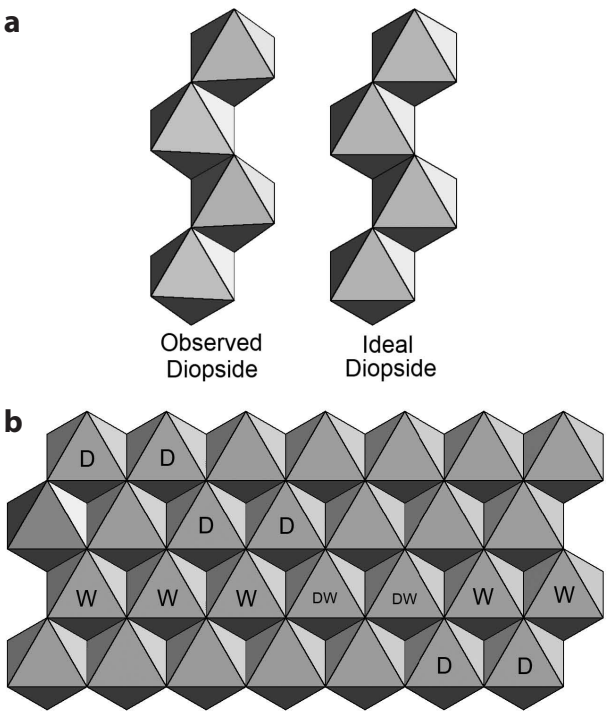


**FIGURE 9.** (**a**) A comparison of the M1 O-chain in observed and ideal diopside (Thompson and Downs 2008) viewed down **a***, with the O-chain running parallel to **c**. Ideal diopside is constrained to have regular polyhedra. (**b**) The ideal wollastonite (labeled "W") and diopside (labeled "D") O-chains placed in the context of a fully occupied closest-packed octahedral layer (brucite-type layer). O-chain orientation in the brucite-type layer is important because it determines the possible orientations of associated T-chains in close-packed minerals.

of the 30° orientations—the other two may be easily visualized from Figures 9a and 9b. These differences are fundamental because they determine how T-chains can be oriented relative to O-chains in close-packed minerals.

O-chains in more complex but still isopolyhedral layer pyroxenoids can be thought of as intermediate between the end-member O-chains of wollastonite and pyroxene. Figures 10a–10c illustrate the relationships between the pyroxene and pyroxenoid O-chains for rhodonite (Peacor et al. 1978), pyroxmangite (Zanazzi et al. 2008), and ferrosilite III (Weber 1983), which have T-chain repeat lengths of 5, 7, and 9, respectively, by placing them in the context of brucite-type layers. Longer T-chain repeat unit lengths correlate with O-chain geometries that are increasingly pyroxene-like. Each time the pyroxenoid T-chain repeat length increases by 2, the number of octahedra overlapping between the pyroxene and pyroxenoid O-chains increases by 2.

As O-chain geometries become increasingly pyroxene-like with increasing T-chain repeat length, so do T:O single chain ratios in isopolyhedral layer pyroxenoids. Table 4 demonstrates that the T:O ratio in these minerals is $x$:($x$ – 1), where $x$ is the

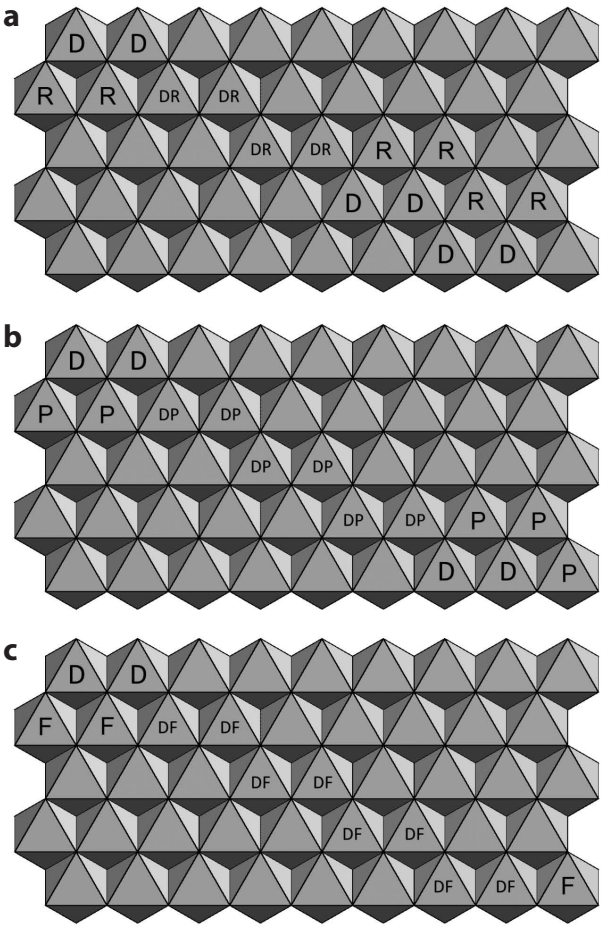


**FIGURE 10.** The relationships between the pyroxene and pyroxenoid O-chains for (**a**) rhodonite (Peacor et al. 1978), (**b**) pyroxmangite (Zanazzi et al. 2008), and (**c**) ferrosilite III (Weber 1983), which have T-chain repeat lengths of 5, 7, and 9, respectively.

T-chain repeat length. The T-chain repeat length increases by 2, the pyroxene T-chain repeat length, in each succeeding row in the table. Correspondingly, the O-chains become increasingly staggered in a fashion that makes them more pyroxene-like and the T:O ratio approaches the pyroxene value of 1:1.

In an ideal closest-packed structure, the octahedral:tetrahedral volume ratio is 4:1. In observed wollastonite, the average ratio is 7.7:1. The large size of the Ca atom is responsible for this large volume ratio, and the large size of the octahedra allows for the 3:2 single-chain T:O ratio. The difference in the T:O ratio between pyroxenes and pyroxenoids is a fundamental structural difference, and another proof that pyroxenoids are not close-packed minerals.

Table 5 lists average M-site cation radius and average O-chain cation radius for the four pyroxenoids discussed so far and for diopside. T-chain repeat length increases and the pyroxenoids become more pyroxene-like as average O-chain cation radius decreases. One can easily imagine a pyroxenoid structure falling in between ferrosilite III and clinopyroxene with the O-chain geometry illustrated in Figure 11 and a T-chain repeat unit of length 11. These structures are related by straightforward intralayer alterations in chain geometry resulting from differences, sometimes relatively small, in chemistry. Ferrosilite III is a high-temperature synthetic. A pyroxenoid with T-chain repeat length of 11 may not exist in nature, but it may be possible to synthesize such a crystal at high temperature if the starting materials contain the correct ratio of Fe and a smaller M cation such as Mg.

By the criteria of this discussion, amphiboles are much more like pyroxenes than are pyroxenoids because their O-chains can be oriented parallel to pyroxene O-chains in a brucite-type layer, they have the pyroxene T-chain repeat unit length of 2, and they have T:O ratios of 1:1 between T-chains and their associated octahedra.

All of the phases so far discussed have general formula $MSiO_3$ and have O-chain geometries that lie somewhere on the wollastonite-pyroxene spectrum. All contain isopolyhedral layers and form the well-known wollastonite-rhodonite-pyroxmangite-ferrosilite III-clinopyroxene series.

However, there is at least one pyroxenoid-like chain silicate that has a different stoichiometry and is related to wollastonite in a different fashion. The new mineral yangite has general formula $M1M2Si_3O_9$, and can be thought of as composed of mixed polyhedral layers that contain both T- and O-sites stacked along face pole ($\bar{1}03$). Yangite's O-chains orient in a brucite-type layer in the same manner as wollastonite, but yangite's M:T formula ratio is two-thirds that of wollastonite and therefore has an octahedral band that is two octahedra wide instead of three as in wollastonite.

Yangite has two related complexities not present in the pyroxenoids discussed so far—double T-chains and layers that are not isopolyhedral. Figure 12a compares a portion of yangite viewed down **b** with a portion of wollastonite viewed down **c**, illustrating the mixed polyhedral layers of yangite vs. the isopolyhedral layers of wollastonite. Yangite's double T-chain connects four octahedral bands of width 2 in four different layers, while wollastonite's single T-chain connects three octahedral bands of width 3 in two different layers.

The two halves of yangite's double T-chains are related by an inversion, making them very different geometrically from amphibole double T-chains, which are related by a mirror. The inversion splits the double chain between polyhedral layers, resulting in the mixed polyhedral layers described above (Fig. 12a). To visualize this, compare the yangite double T-chains (Fig. 12a) with the top half of Figure 12b, which illustrates the amphibole double T-chain using obertiite (Hawthorne et al. 2000) as an exemplar.

Each half of the yangite double T-chain (i.e., each component single chain) performs the same structural function as the pyroxenoid single T-chain, the pyroxene single T-chain, and the amphibole double T-chain. Each of these components connects to two linear structural subunits in one of the adjacent polyhedral layers and to one in other adjacent polyhedral layer. In the case of the pyroxenoids, pyroxenes, and amphiboles, these linear subunits are all octahedral bands. In the case of yangite, one of them is a single T-chain (half of the double T-chain). To see

**TABLE 4.** The single-chain T:O ratio in several isopolyhedral layer pyroxenoids

| Mineral | T-chain repeat length | T:O | Reference |
|---|---|---|---|
| Wollastonite | 3 | 3:2 | Ohashi and Finger (1978) |
| Rhodonite | 5 | 5:4 | Peacor et al. (1978) |
| Pyroxmangite | 7 | 7:6 | Zanazzi et al. (2008) |
| Ferrosilite III | 9 | 9:8 | Weber (1983) |
| | *x* | *x*:(*x* – 1) | |
| Diopside | 2 | 1:1 | Thompson and Downs (2008) |

*Note:* As the T-chain repeat length increases, the ratio approaches the pyroxene value of 1:1.

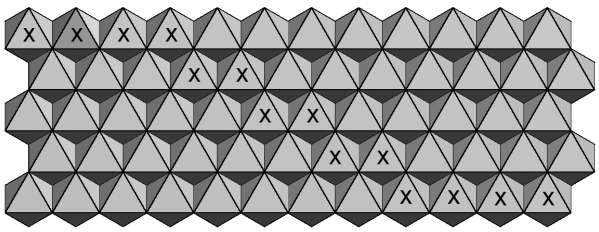


**FIGURE 11.** The O-chain geometry in the context of a brucite-type layer of a hypothetical pyroxenoid with a T-chain repeat unit length of 11.

**TABLE 5.** The single-chain T:O ratio in several isopolyhedral layer pyroxenoids

| Mineral | T-chain repeat length | Avg. M-site cation radius (Å) | Avg. O-chain cation radius (Å) | Reference |
|---|---|---|---|---|
| Wollastonite | 3 | 0.99 | 0.99 | Ohashi and Finger (1978) |
| Rhodonite | 5 | 0.83 | 0.85 | Peacor et al. (1978) |
| Pyroxmangite | 7 | 0.82 | 0.79 | Zanazzi et al. (2008) |
| Ferrosilite III | 9 | 0.78 | 0.78 | Weber (1983) |
| Diopside | 2 | 0.86 | 0.72 | Thompson and Downs (2008) |

*Notes:* As the T-chain repeat length increases, the ratio approaches the pyroxene value of 1:1. Average M-site cation radius is calculated assuming sixfold-coordination. Radii are from Shannon (1976).

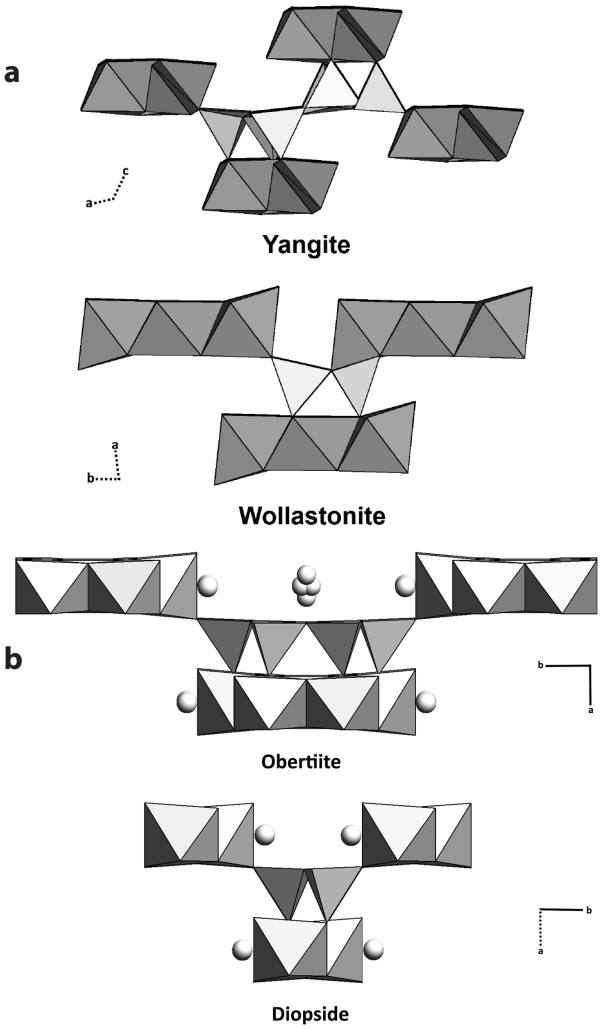


**FIGURE 12.** (**a**) A comparison of yangite (Downs et al. 2016) viewed down **b** with wollastonite-1*A* (Ohashi and Finger 1978) viewed down **c**. (**b**) A comparison of amphibole (obertiite, Hawthorne et al. 2000) with clinepyroxene (diopside, Thompson and Downs 2008), both viewed down **c**.

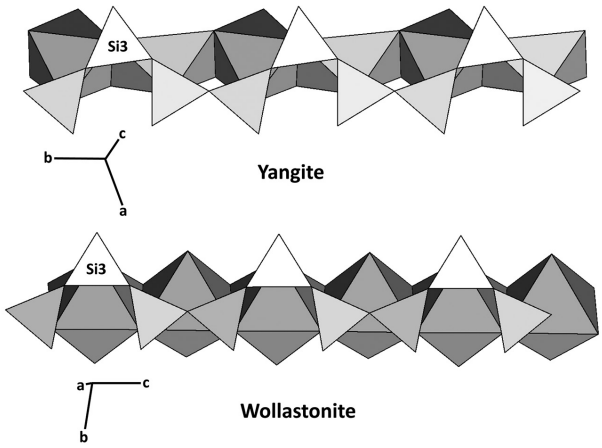


**FIGURE 13.** A comparison of half of the yangite double T-chain viewed down face pole ($\bar{1}03$) with the wollastonite T-chain (Ohashi and Finger 1978) viewed down **a*** showing their identical tetrahedral geometries, but opposite orientations relative to the octahedra.

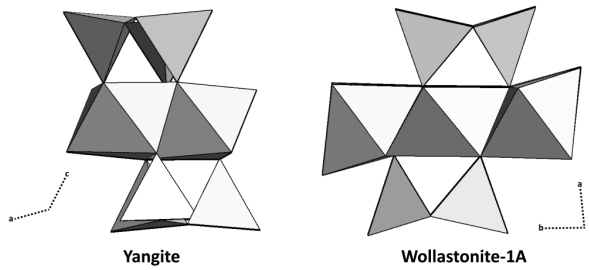


**FIGURE 14.** The I-beams of yangite (Downs et al. 2016) and wollastonite-1*A* (Ohashi and Finger 1978).

this, imagine removing the uppermost and rightmost octahedral bands in the yangite illustration of Figure 12a. With that image in mind, the central T-chain in all four of the Figure 12 diagrams is functionally the same.

Yangite exhibits the 3:2 single-chain T:O ratio characteristic of wollastonite along with its T chain repeat length of 3. Figure 13 illustrates this similarity. It also highlights an important difference between yangite and wollastonite: the orientation of the yangite T-chain relative to its associated O-chain is opposite that of wollastonite. To see this, observe that the visible face of the yangite T3 tetrahedron and the approximately parallel faces of its two associated octahedra point in opposite directions; but in wollastonite, the visible T3 tetrahedral face points in the same direction as the parallel face of its associated octahedron.

Pyroxenes and pyroxenoids are often described as composed of interconnected "I-beams" (cf. Papike et al. 1973), a structural subunit consisting of an octahedral band sandwiched between two single-T chains. Figure 14 contrasts the yangite and wollastonite-1*A* I-beams. There are important differences between the manner in which I-beams are connected in the two minerals. The yangite I-beam is connected to four other I-beams and has a T-T connection (to the other half of the double T-chain), while the wollastonite I-beam is connected to six other I-beams and only through T-O connections. The yangite I-beams connects to other I-beams through bridging O atoms, but the wollastonite octahedral band shares edges with some tetrahedra in other I-beams. Yangite has no connections to other I-beams at the northeast and southwest corners of the octahedral band pictured in Figure 14, while the wollastonite octahedral band is connected at all four corners.

These differences are evident in Figure 15, which shows how the octahedral bands connect to other I-beams at the northwest and southeast corners as pictured in Figure 14. The tetrahedra in Figure 15 belong to neighboring I-beams and not the I-beam that includes the pictured octahedral band, whose tetrahedra have been removed from the image. Each illustrated T-chain segment contains 2 three-tetrahedron repeat units. The opposite orientation of the T-chains relative to the octahedral bands in yangite and wollastonite described above is again evident here and requires different I-beam connectivity.

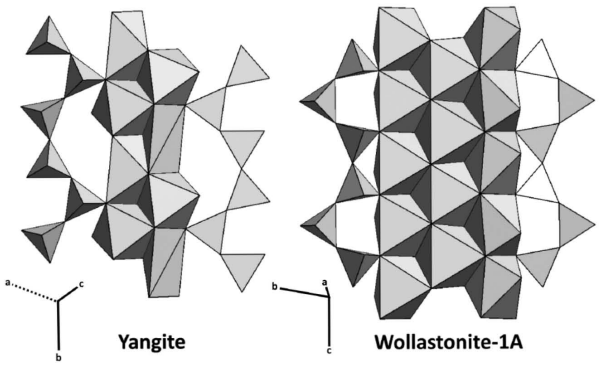


**Figure 15.** Segments of the octahedral bands of yangite (Downs et al. 2016) and wollastonite-1*A* (Ohashi and Finger 1978) along with T-chains from different I-beams.

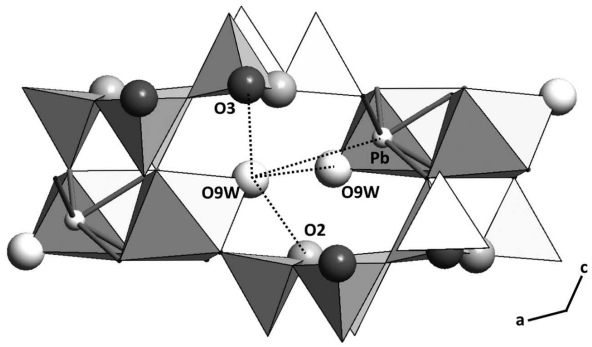


**Figure 16.** A portion of the yangite structure viewed down **b**, showing possible hydrogen bonds (dotted lines) bridging and perhaps stabilizing a channel in the structure.

Definitions of the term "pyroxenoid" often include a single T-chain as a defining characteristic. This definition precludes yangite from classification as a pyroxenoid. Yangite and the pyroxenoids bear more similarity to each other than either does to any other mineral species or group. Reasonable arguments could be made to expand the definition of "pyroxenoid" so that it includes yangite, coin the term "amphiboloid" and count yangite as this new group's first member (as suggested by one reviewer), or leave it on its own.

Downs et al. (2016) present yangite in a setting that corresponds with the predicted structure of Merlino and Bonaccorsi (2008), and that is the setting used in the figures herein. The conventional settings for pyroxenes and pyroxenoids puts **c** parallel to the octahedral bands and T-chains and the stacking vector parallel to **a***. A large cell is required to place yangite in a corresponding setting, with cell parameters[$\mathbf{a}'$, $\mathbf{b}'$, $\mathbf{c}'$, $\alpha'$, $\beta'$, $\gamma'$] = [$c$, $3a + b + c$, $b$, $a\cos([311]\cdot b/|[311]|\cdot b)$, $\alpha$, $a\cos([311]\cdot \mathbf{c}/|[311]|\cdot c)$] and positional parameters [x′, y′, z′] = [–x/3 + z, x/3, –x/3 + y]. A simpler transformation, [$\mathbf{a}'$, $\mathbf{b}'$, $\mathbf{c}'$, $\alpha'$, $\beta'$, $\gamma'$] = [$c$, $a$, $b$, $\gamma$, $\alpha$, $\beta$] and [x′, y′, z′] = [z, x, y], puts **c** parallel to the octahedral bands and T-chains, but does not put the stacking vector parallel to **a***, and therefore is not as useful for structural comparisons.

Yangite was refined without locating the hydrogen atoms (Downs et al. 2016). The refinement leaves O9W dangling, bonded only to Mn (Fig. 16), an extremely unusual topology. The fact that O9W is a water molecule may be enough to stabilize the structure, but the presence of hydrogen bonds is likely. Any such hydrogen bonds cannot be located with certainty, but a range of possibilities can be described.

Procrystal electron density calculations (cf. Downs et al. 2002 for a description of the method and its efficacy) indicate weak O9W-O2, O9W-O3, O9W-O9W, O9W-Pb bonds (Downs et al. 2016). Figure 16 illustrates these bond paths. There are two more bonds than hydrogen atoms because stabilizing O-O bonds may exist without the presence of hydrogen bonding (cf. Pakiari and Eskandari 2007). We rule out the O9W-O9W bond path as a location for hydrogen atoms because a single hydrogen along this path violates the crystal's symmetry. Although stabilizing H-H bonds for nearly electrically neutral hydrogen atoms in organic molecules have been reported (Matta et al. 2003), we also rule out two hydrogen atoms along the O9W-O9W path based on crystal chemistry.

There are three remaining possible pairs of hydrogen bonds: O9W-O2 and O9W-O3, O9W-O2 and O9W-Pb, or O9W-O3 and O9W-Pb, with no solid criteria for choosing among them. The O9W-Pb bond path is an intriguing possibility given lead's lone pair of electrons. Unfortunately, there is not enough yangite sample to propose a neutron diffraction study to locate its hydrogen atoms, but the possibility of an O-Pb hydrogen bond is sufficiently interesting that a search for a similar crystal chemical environment in a more abundant compound is worthwhile.

## Implications

Several lines of evidence demonstrate that while pyroxenes are based on close-packing of oxygen atoms, pyroxenoids are not. This is a profound structural difference and is the result of the characteristic pyroxenoid T-chain/O-chain geometry. Specifically, every pyroxenoid T- and associated O-chain contains at least a segment in which the T:O single chain ratio is 3:2, a geometry incompatible with close-packing. Pyroxenoid packing arrangements and relationships with pyroxenes cannot be fully understood through T-chain analysis alone; O-chain geometries provide fundamental insights because O-chain chemistry varies between pyroxenoids while T-chains are always composed of $SiO_4$ tetrahedra.

Because the octahedral chains of both pyroxenes and pyroxenoids can be placed in the context of a close-packed brucite-type layer, O-chains are ideal for analyzing the relationships between pyroxenes and pyroxenoids. Such analysis shows that as the average O-chain cation size decreases, O-chain geometry (and therefore the T:O single chain ratio) becomes increasingly staggered and pyroxene-like in predictable fashion. One can therefore easily predict what the O-chain in an isopolyhedral layer pyroxenoid with T-chain repeat length 11 (or more) will look like if and when such a mineral is discovered or crystal synthesized.

Additionally, because octahedral bands in pyroxenoids when considered in isolation have close-packed arrangements of O atoms, they must distort considerably to accommodate the non-closest-packed T-chains to which they are connected.

The existence of a pyroxenoid-like crystal with mixed polyhedral layers, yangite, suggests that the number of possible

structures closely related to the pyroxenoids is much larger than previously thought and that new minerals with novel related structures will continue to be discovered.

Pyroxenoids can be classified in several new ways: O-chain geometry, single-chain T:O ratios, mixed vs. isopolyhedral layers, and single vs. double (or perhaps more) T-chains.

## Acknowledgments

We thank an anonymous reviewer, Fernando Cámara, and associate editor Fernando Colombo, whose comments greatly improved the quality of this manuscript. We particularly appreciate F. Cámara's extensive edit and the time it must have required.

## References cited

Angel, R.J., and Burnham, C.W. (1991) Pyroxene-pyroxenoid polysomatism revisited: A clarification. American Mineralogist, 76, 900–903.

Downs, R.T., Gibbs, G.V., Boisen, M.B. Jr., and Rosso, K.M. (2002) A comparison of procrystal and ab initio model representations of the electron-density distributions of minerals. Physics and Chemistry of Minerals, 29, 369–385.

Downs, R.T., Pinch, W.W., Thompson, R.M., Evans, S.H., and Megaw, L. (2016) Yangite, $PbMnSi_3O_8 \cdot H_2O$, a new mineral species with double wollastonite silicate chains, from the Kombat mine, Namibia. American Mineralogist, 101, 2539–2543.

Hawthorne, F.C., Cooper, M.A., Grice, J.D., and Ottolini, L. (2000) A new anhydrous amphibole from the Eifel region, Germany: Description and crystal structure of obertiite, $NaNa_2(Mg_3FeTiSi_8O_{22}O_2$. American Mineralogist, 85, 236–241.

Klein, C., and Dutrow, B. (2008) The Manual of Mineral Science. Wiley.

Liebau, F. (1956) Bemerkungen zur systematik der kristallstrukturen von silikaten mit hochkondensierten anionen. Zeitschrift für physikalische Chemie 206, 73–92.

Matta, C.F., Hernández-Trujillo, J., Tang, T.-H., and Bader, R.F.W. (2003) Hydrogen-hydrogen bonding: A stabilizing interaction in molecules and crystals. Chemistry—A European Journal, 9, 1940–1951.

Merlino, S., and Bonaccorsi, E. (2008) Double wollastonite chains: Topological/conformational varieties, polytypic forms, isotypic compounds. Zeitschrift für Kristallographie, 223, 85–97.

Ohashi, Y., and Finger, L.W. (1978) The role of octahedral cations in pyroxenoid crystal chemistry. I. Bustamite, wollastonite, and the pectolite-schizolite-serandite series. American Mineralogist, 63, 274–288.

Pakiari, A.H., and Eskandari, K. (2007) Closed shell oxygen-oxygen bonding interaction based on electron density analysis. Journal of Molecular Structure: THEOCHEM, 806, 1–7.

Papike, J.J., Prewitt, C.T., Sueno, S., and Cameron, M. (1973) Pyroxenes: Comparisons of real and ideal structural topologies. Zeitschrift für Kristallographie, 138, 254–273.

Peacor, D.R., Essene, E.J., Brown, P.E., and Winter, G.A. (1978) The crystal chemistry and petrogenesis of a magnesian rhodonite. American Mineralogist, 63, 1137–1142.

Prewitt, C.T., and Peacor, D.R. (1964) Crystal chemistry of the pyroxenes and pyroxenoids. American Mineralogist, 49, 1527–1542.

Ried, H. (1984) Intergrowth of pyroxene and pyroxenoid; chain periodicity faults in pyroxene. Physics and Chemistry of Minerals, 10, 230–235.

Robinson, K., Gibbs, G.V., and Ribbe, P.H. (1971) Quadratic elongation: a quantitative measure of distortion in coordination polyhedra. Science, 172, 567–570.

Shannon, R.D. (1976) Revised effective ionic radii and systematic studies of interatomic distances in halides and chalcogenides. Acta Crystallographica, A32, 751–767.

Thompson, J.B. (1970) Geometrical possibilities for amphibole structures: Model biopyriboles. American Mineralogist, 55, 292–293.

Thompson, R.M., and Downs, R.T. (2003) Model pyroxenes I: Ideal pyroxene topologies. American Mineralogist, 88, 653–666.

——— (2008) The crystal structure of diopside at pressure to 10 GPa. American Mineralogist, 93, 177–186.

Veblen, D.R. (1991) Polysomatism and polysomatic series: A review and application. American Mineralogist, 76, 801–826.

Weber, H.-P. (1983) Ferrosilite III, the high-temperature polymorph of $FeSiO_3$. Acta Crystallographica, C39, 1–3.

Zanazzi, P.F., Nestola, F., Nazzareni, S., and Comodi, P. (2008) Pyroxmangite: A high pressure single-crystal study. American Mineralogist, 93, 1921–1928.

Manuscript received January 13, 2016
Manuscript accepted June 27, 2016
Manuscript handled by Fernando Colombo